See p 13/10

PAPER 13 (SESSION I)

The effect of thickness and drilled holes on the notch-toughness of Charpy V-notch bars

C. A. RAU, Jr.* and Prof A. S. TETELMAN †

* Pratt & Whitney Aircraft, AMRDL, Middletown, Connecticut, U.S.A.
† Department of Engineering, U.C.L.A., Los Angeles, California, U.S.A.

Summary

Instrumented Charpy tests were performed over a wide range of temperatures on 0·394 in, 0·200 in, and 0·100 in thick samples of Fe-3% Si and mild steel. Some of these samples contained two small holes, drilled through the thickness near the notch tip. From dynamic load-time curves, the increase of triaxial constraint prior to general yield and the mechanisms of plane strain relaxation after general yield were quantitatively defined for both undrilled and drilled bars of each thickness. For undrilled samples, the results indicate that thinner bars have up to 50% greater notch strength at low temperatures where all samples cleave prior to general yielding, and that the nil-ductility transition temperature decreases markedly with decreasing thickness (as much as 80°C). These two improvements in thinner bars result from the reduced rate at which triaxiality builds up with applied load and the lower maximum constraint obtained at general yield, respectively. After general yielding, relaxation of constraint by through-thickness (plane stress) deformation occurs at smaller bend angles in thinner samples. Consequently, the ductility transition temperature, defined by a sharp rise in fracture strength and toughness, decreases with decreasing thickness but not at the same rate as the nil-ductility temperature. Two drilled holes produce comparable improvements in both the low temperature strength and transition behavior in each of the thicknesses investigated. The means by which holes reduce the triaxiality in thinner samples is discussed quantitatively, in terms of the combination of plane strain relaxation mechanisms which operate and the thickness dependence of each.

Introduction

Fracture mechanics studies [1-4] on sharply cracked specimens of high yield strength materials have shown that at a given temperature, decreasing thickness causes the fracture toughness K_C to increase from its lower limiting value K_{IC}; and the fracture appearance to change from the completely flat (opening) mode to a mixture of the opening and shear lip (45°) modes. Similarly, the notch impact transition temperature of mild steel, as defined by a sharp rise in impact energy or non-crystalline fracture, decreases with decreasing specimen thickness [5-8]. These beneficial effects of decreasing thickness are generally ascribed to a decrease in plane strain triaxial constraint, at a given plastic zone size before general yield or nominal strain after general yield, but no quantitative study of the effect of thickness on triaxial constraint has been reported. The first purpose of the present investigation was to define the effect of specimen thickness on the build-up of triaxial constraint with

increasing local deformation and the maximum possible constraint, in notched bars of mild steel and Fe-3% Si, tested in a temperature range where fracture occurs by complete cleavage without shear lip formation. The results on the Fe-3% Si are also used to show that even in a completely clean, single phase material, local tensile stresses play a significant role in the fracture process and that fracture models based on a critical shear stress for crack nucleation are incomplete.

Previously [9, 10], we have shown that two small holes, appropriately drilled around the V-notch, are able to reduce the Charpy impact transition temperature (by 50 °C) and increase the notch bar fracture strength at low temperatures, in specimen of standard thickness (0·394 in). The second purpose of the present investigation was to determine whether further beneficial effects on toughness could be achieved through a combination of reduced thickness and hole drilling. We have indeed found that this combination was able to cause a reduction in transition temperature by as much as 100 °C. An analysis of the data indicates that this combination is effective because the holes reduce constraint through a change in the in-plane, plane strain deformation mode, while the reduced thickness induces a change in deformation mode from plane strain to plane stress.

Experimental procedure

The two materials used in this study are described below in Table 1.

Table 1

Alloy	*C*	*Mn*	*Si*	*Ni*	*P*	*S*	*Grain size* (10^{-3} *in*)	*Condition*
Steel 0·24	0·24	0·47	0·031	–	0·007	–	0·8	Hot rolled
Fe-Si	0·01	–	3·25	–	–	–	21·0	Annealed

Steel 0·24 is a fine-grained, commercial mild steel consisting of 25 volume percent pearlite colonies and some semi-continuous carbides at ferrite grain boundaries; the Fe-Si is a coarse-grained, single phase material.

All specimen dimensions were those of the standard V-notch Charpy except the thickness (t) as specified. Drilled specimens contained two 0·0292 in diameter holes, located as shown in Fig. 3. Each thickness was prepared by grinding equal amounts from top and bottom of a ½ in plate so that in each thickness the specimen center coincided with the plate center. The notch was cut transverse to the rolling direction, and holes were drilled prior to vacuum annealing of Fe-Si for one hour at

875 °C. Steel samples were tested in the hot rolled condition. Impact-bend tests were performed on a Wiedemann-Baldwin, SI-1, 240 ft lb machine (17 ft/sec impact velocity) whose pendulum striker was specially instrumented to record the load applied to the bar during the test. The instrumentation was similar to that used by others [11-17] and is described elsewhere [10, 18] along with the calibration procedure which was performed for each thickness bar. For this study, the instrumented Charpy test provided distinct advantages over slow-bend tests. First, the transition region of both materials is raised to higher temperatures so that the region where failure occurs prior to general yield could be studied extensively. Second, the temperature dependence of the flow stress is reduced markedly at high strain rates, thereby spreading the region of interest over a wider temperature range.

At approximately ½ ° increments of plastic bend angle, slow-bend samples were unloaded, and the change in thickness was measured by both interferometry and a calibrated microscope. Specifically, a partially reflective optically flat glass was placed over each deformed bar and 20 × photographs were taken with monochromatic sodium light ($\lambda = 5985$ Å). Interference of light reflected from the specimen surface with that from the flat produced fringes which were reduced to the surface normal displacements by a straightforward calculation which accounts for the linear tilt of the optical flat. At bend angles greater than 4 °, fringes became too close together to count conveniently. By using a calibrated specimen stage (0·001 mm per division) on a Leitz microscope and focusing at various points below the notch, contraction measurements were obtained at bend angles up to 10 °.

Experimental results

A. *Fracture studies on standard samples of varying thickness*

Figs. 1 and 2 summarize the yield and fracture behavior of 0·100 in, 0·200 in, and standard 0·394 in thick notched samples at various test temperatures. Normalizing all results to the standard Charpy area, reduced thickness produces the following changes:

(1) The notch strength of thinner samples is up to 50% greater than standard Charpys at low temperatures, where all samples cleave prior to general yielding.

(2) The nil-ductility temperature, where fracture occurs just at general yielding, T_D (see Fig. 3), decreases with decreasing thickness as summarized in Table 2.

(3) Above the nil-ductility temperature, general yielding precedes fracture, but cleavage occurs at small bend angles until the ductility transition temperature (T_N) is reached, where the bend angle increases markedly prior to failure. Table 2 summarizes the effect of thickness on

the two transition temperatures. In mild steel, the ductility transition was always accompanied by a change in fracture initiation mode from cleavage to fibrous tearing. In 0·2 in thick Fe-Si, however, fracture occurred by 100% cleavage both above and below the ductility transition. In 0·1 in thick Fe-Si, cleavage was not observed above T_N.

(4) The normalized general yield loads (P_{GY}) of 0·200 in and 0·100 in samples are nearly identical and 6-8% below that of the standard thickness (0·394 in) samples.

Table 2

The effect of two 0·0292 in holes on the impact transition temperatures, general yield load, and ultimate load of various thickness samples of mild steel and Fe-Si

		Mild steel			*Fe-Si*		
		t = 0·394 in	*t* = 0·200 in	*t* = 0·100 in	*t* = 0·394 in	*t* = 0·200 in	*t* = 0·100 in
Nil-ductility	T_D^t	−15	−30	−60	90	15	10
Temperature	T_{DH}^t	−55	−76	−102	40	−20	−15
(°C)	ΔT_D^t	−40	−46	−42	−50	−35	−25
Ductility	T_N^t	+10	−10	−40	90	60	40
Transition temperature	T_{DN}^t	−50	−55	−90	60	45	0
(°C)	ΔT_N^t	−60	−45	−50	−30	−15	−40
Fracture to both holes (°C)	T_{NH}'	−50	−45/−60	−55	60	60	60
Change in general yield load (%)	ΔP_{GY}	−11	−7	−7	−11·5	−9	−9
Change in ultimate load (%)	$\Delta P_{ult.}$	−8·5	−4	−4·5	−9	−8	−7·5

(5) At higher temperatures where specimens of all thicknesses are ductile, plastic instability occurs at a smaller plastic bend angle and correspondingly lower ultimate load in thinner samples.

B. *Fracture studies on drilled samples of varying thickness*

1. *Standard thickness (t = 0·394 in)*

Fig. 3 compares the fracture results of standard thickness mild steel Charpy samples with those containing two 0·0292 in diameter holes. The significant changes resulting from the introduction of holes are as follows:

(1) At very low temperatures ($T < 140$ °C), drilled samples are only 10% stronger than standard Charpys. Fracture occurs by 100% cleavage at less than 30% of the extrapolated general yield load.

(2) Between −140 °C and −40 °C, the fracture strength of drilled samples increases much more rapidly with temperature than does the strength of standard samples. Consequently, the load carrying capacity of drilled samples is up to 70% higher than that of standard bars even though both cleave prior to general yielding. In this temperature range, the fracture path in drilled samples may include one hole or neither hole with similar improvements observed in either case.

(3) Two holes reduce both the nil-ductility and ductility transition temperatures significantly as summarized in Table 2. The ductility transition of drilled bars results when shear failure occurs between the notch sides and both holes. The notch then has two tips in the form of elongated holes from which reinitiation of fracture is much more difficult [9]. Holes did not change the amount of post-brittle (shear-lip) energy so that the total Charpy energy is proportional to the plastic bend angle.

(4) Both the general yield and ultimate loads of drilled bars are 5-10% below those of standard Charpy specimens at all temperatures.

2. *Thinner samples (t = 0·200 in, 0·100 in)*

(1) At low temperatures, two holes drilled in thinner bars improve the notch strength by the same relative magnitudes obtained in the standard thickness.

(2) Holes reduce the nil-ductility temperatures by similar amounts in all thicknesses as summarized in Table 2.

(3) Holes reduce the ductility transition temperature, but the magnitude depends on thickness and the alloy (Table 2).

(4) At a higher temperature where shearing occurs between the notch and both holes, there is a second sharp increase in the fracture energy. The temperature (T_N', Table II) at which this occurs is nearly independent of thickness.

(5) Both the general yield and ultimate load of thinner samples are reduced by two holes. The magnitudes of the reductions (5-10%) are

similar to those produced in standard thickness bars, but they decrease slightly with decreasing thickness as shown in Table 2.

C. *Transverse displacement measurements*

In all thicknesses, contraction of plain notched bars is a maximum at the notch tip and decreases monotonically (roughly linearly) to zero at approximately 3·5 mm below the notch (neutral axis). In drilled bars, the maximum contraction also occurs at the notch root, but there is a region between four and eight root radii below the notch (1-2 mm) where the contraction increases slightly with distance from the notch before decreasing to zero at 3·5 mm below the notch.

In order to evaluate the effect of variations in thickness, notch contraction was converted to *average* transverse strain by dividing by the thickness. The effect of thickness and holes on the average transverse strain at a point 2 root radii below the notch tip is summarized in Fig. 4 (above general yield) and Fig. 6 (below general yield). In both standard and drilled samples, the average transverse strains increase nearly linearly with plastic bend angle after general yield (0·6°). At corresponding bend angles, the transverse strains are considerably higher in plain bars of reduced thickness. However, two holes have little effect on the average transverse strain prior to general yielding (Fig. 6), and they actually reduce the average transverse strains beyond general yielding (Fig. 5).

Discussion

A. *Fracture before general yielding*

Initial yielding occurs when the applied nominal stress (σ_N), raised locally by elastic stress concentration factor (4·2), exceeds the uniaxial yield stress at the notch tip (σ_Y^*). That is, when

$$\sigma_N = \frac{\sigma_Y^*}{4{\cdot}2} \tag{1}$$

In three point bending of the Charpy bar the applied load (P_{LY}) to produce yielding is calculated from the simple beam formula (10), P_{LY} (lb)= $3{\cdot}9\times10^{-3}\ \sigma_Y^*$ (psi). For applied loads greater than P_{LY}, plastic zones in a perfectly plastic material develop in the form of logarithmic spirals, producing longitudinal stresses σ_{yy} within the plastic zone which are given by Hill [19]

$$\sigma_{yy}(x) = \sigma_Y^*\left[1 + \ln\left(1 + \frac{x}{\rho}\right)\right] \tag{2}$$

where x is the distance below the notch root and $\rho=0{\cdot}010$ in is the radius of curvature of the notch root. The maximum tensile stress occurs at the elastic-plastic interface $x=R$ and is given by

$$\sigma_{yy}^{max} = \sigma_Y^*\ K_{\sigma(p)}$$
$$K_{\sigma(p)} \equiv 1 + \ln(1 + R/\rho) \tag{3}$$

where $K_{\sigma(p)}$ is the plastic stress concentration factor, and $R \equiv R(P/\sigma_Y^*)$ is the plastic zone size, which depends on the applied load and yield stress [20, 21].

Hill [19] has shown that there is a plastic zone size beyond which $K_{\sigma(p)}$ no longer increases, and Green and Hundy [22] have theoretically calculated the maximum value of $K_{\sigma(p)}$ to be

$$K_{\sigma(p)}^{max} \equiv 1 + \frac{\pi}{2} - \frac{\omega}{2} = 2{\cdot}18 \tag{4}$$

for the Charpy notch. Recently, Ewing [23] has shown that equation (4) is not strictly applicable to the Charpy geometry. His more exact calculations show the actual value of $K_{\sigma(p)}^{max}$ for the Charpy bar is 1·95.

Low temperature cleavage fracture occurs in notched specimens of mild steel and Fe-Si when an unstable microcrack is nucleated ahead of the notch and grows into a fast running macrocrack. Various investigators [21, 24-27] have shown that in mild steel this occurs when the maximum tensile stress σ_{yy}^{max} exceeds a critical value (σ_f^*) which is roughly independent of temperature. The low temperature cleavage fracture criterion for a notched bar is therefore given by

$$\sigma_{yy}^{max} = \sigma_Y^*\ K_{\sigma(p)}^F = \sigma_f^*$$

or

$$K_{\sigma(p)} = K_{\sigma(p)}^F(T) = \frac{\sigma_f^*}{\sigma_Y^*(T)}\Bigg/ \text{at } P/\sigma_Y^* = P_F/\sigma_Y^* \tag{5}$$

The critical plastic stress concentration factor $K_{\sigma(p)}^F$ must increase with temperature as $\sigma_Y^*(T)$ decreases, in order to satisfy equation (5); consequently the critical plastic zone size increases with temperature.

In previous work with this mild steel [10], the dynamic yield stress $\sigma_Y^*(T)$ was generated as a function of temperature and used to calculate $\sigma_f^* = 174{,}000$ psi from instrumented Charpy results. Substituting σ_f^* and σ_Y^* for each temperature into equation (5) yields the critical stress intensification required to cause cleavage at each temperature, $K_{\sigma(p)}^F(T)$. The experimental fracture loads at corresponding temperatures thus

define directly the increase of $K_{\sigma(p)}$ with applied load for the geometry tested. A similar procedure has been used by Hahn and Rosenfield [28] to analyze sharply cracked plates and by Knott [29] to analyze V-notched bars.

The plastic stress concentration factors for the various thickness, plain and drilled bars were developed in this way† and are summarized in Fig. 5. No attempt is made to distinguish between stress intensification by plastic constraint and that which may result from local strain hardening, since the steel is not ideally plastic. However, the latter contribution is believed small prior to general yielding, as evidenced by the agreement between the experimentally measured maximum constraint (2·01) and that calculated by Ewing [23] for an ideal plastic Charpy bar (1·95). Furthermore, for applied loads up to half that for general yielding, constraint in the standard Charpy bar agrees very well with that predicted theoretically by Wilshaw, Rau, and Tetelman [21] for an ideal plastic materia

It is apparent that constraint builds up less rapidly with applied load in thinner bars, and consequently, at a given temperature, a higher load is required to achieve the necessary degree of local stress intensification to cause fracture. To the best of our knowledge, this is the first *direct* evidence that the fracture toughness can be altered, by decreasing thickness, even though the fracture is 100% flat cleavage. Furthermore, the data shown in Fig. 2 is the first to show that even in clean, single phase materials such as Fe-3% Si, local constraint and hence local *tensile* stresses play a key role in the fracture processes. This indicates that recent dislocation models [30-32], that purport to show that microcrack nucleation under shear stress *alone* is the critical step in the fracture process in single phase solids, are incorrect.

The effect of holes, thickness, or any other geometrical change is to either (1) modify the in-plane (plane strain) strain distribution or (2) promote relaxation of plane strain conditions. Thus we may separate the plastic stress concentration factor

$$K^{t}_{\sigma(p)} = K^{\infty}_{\sigma(p)} \cdot \chi(t,R) \qquad (6)$$

where $K^{\infty}_{\sigma(p)}$ is the plastic stress concentration factor under fully plane strain conditions, and $\chi \leqslant 1$ represents the degree of relaxation of transverse stresses. Assuming that the 0·394 in bars deform in fully plane strain before general yield ($K^{\infty}_{\sigma(p)} = K^{.394}_{\sigma(p)}$), the decrease of χ with applied load for thinner bars was calculated from Fig. 5 using equation 6. The results, shown in Fig. 6, indicate that relaxation of transverse stresses increases ($\chi\downarrow$) with applied load and is more extensive in thinner bars. The measured transverse strains at corresponding applied loads are also plotted on Fig. 6. They indicate significant plane stress deformation prior to general yield in reduced thicknesses. Also the general yield load itself decreases slightly with decreasing thickness, reflecting lower average constraint across the minimum section analogous to the lower maximum constraint.

† Recently, Radon and Turner [17] have shown that some of the load applied by the pendulum striker is absorbed by specimen inertia. The load at the pendulum, therefore, overestimates slightly the static load required to produce $K^{F}_{\sigma(p)}$. A small correction factor has been applied to the fracture loads (a maximum of 15% at the lowest temperature, decreasing to zero at general yield) in developing Fig. 5 from the fracture loads.

Two holes also reduce the rate at which $K_{\sigma(p)}$ increases with applied load, and their effect is significantly greater than that of thickness alone. Previous photoelastic and dislocation etch-pit results [33] have shown that two holes have very little effect on the *elastic* stress concentration factor and the *initial* plastic zone. Consequently, holes do not affect the initial build up of constraint, and little improvement in notch strength is observed at very low temperatures. With continued loading, however, two holes were shown to cause a marked redistribution of plastic strain away from the notch tip, and thereby holes retard the build up of $K_{\sigma(p)}$ as shown in Fig. 5. At that time, it was not known whether holes enhanced the relaxation of plane strain conditions by promoting through-the-thickness deformation or directly reducing the inplane strain constraint. The similar improvements in notch strength of drilled samples now observed in reduced thicknesses, imply that *holes affect primarily the in-plane strain distribution.* This is substantiated by the direct observation (Fig. 6) that the average transverse strain ahead of the notch is not significantly increased by holes in any thickness while $K_{\sigma(p)}$ is decreased markedly. Assuming then that $\chi(R,t)$ in a drilled bar is the same as that in a plain bar of the same thickness, the plane strain constraint, $K^{\infty}_{\sigma(p)}$, was calculated from Fig. 5 for each thickness. The results, included in Fig. 6, confirm that $K^{\infty}_{\sigma(p)}$ reflects the in-plane strain distribution which is nearly thickness independent prior to general yield.

The notched bar remains nominally elastic until the plastic zones extend across the entire bar at general yielding. The maximum constraint present at this point depends on geometry, as indicated on Fig. 5, and determines the nil-ductility temperature through equation (5). For constant σ_f^* and σ_Y^* varying linearly with temperature, the reduction in transition temperature due to any geometric change 1 → 2 is given [10] by

$$\Delta T_D = T_D^2 - T_D^1 = \frac{[K^{\max,1}_{\sigma(p)} - K^{\max,2}_{\sigma(p)}]}{K^{\max,1}_{\sigma(p)} \; K^{\max,2}_{\sigma(p)}} \frac{\sigma_f^*}{d\sigma_Y^*/dT} \qquad (7)$$

Substitution of the appropriate maximum constraint values into equation (7) permits a good prediction of the effects of both thickness and holes as summarized in Table 2.

Previously, Knott [5] has attempted to estimate the effect of bar thickness on $K^{max}_{\sigma(p)}$ by matching the transition temperatures of thin bars with those of thick bars of variable notch flank angle. He assumed that $K^{max}_{\sigma(p)}$ was given by equation (4); however, Ewing's [23] calculations, as well as the present results, indicate that equation (4) overestimates the actual constraint even for an ideal plastic material. Consequently, Knott's values of $K^{max}_{\sigma(p)}$ are uncertain and much higher than those obtained in this work.

B. *Fracture beyond general yield*

Above the nil ductility temperature the yield stress has decreased so much that the maximum constraint alone does not produce sufficient stress in ...ification to reach the cleavage stress [i.e., $K^{max}_{\sigma(p)} < K^{F}_{\sigma(p)}$ equation (5)]. Some strain hardening [$\Delta\sigma = (d\sigma/d\epsilon)\,\epsilon$] at the point of maximum constraint ($R_\beta = 2{\cdot}25\,\rho$ for V-notch) must increase the flow stress to cause fracture. If neither the maximum constraint nor σ_f^* changes with plastic strain, we may write as a first approximation

$$K^{max}_{\sigma(p)}\left(\sigma_Y^* + \frac{d\sigma}{d\epsilon}\epsilon_f\right) \cong \sigma_f^* \tag{8}$$

so that, the strain required to initiate fracture at R_β is

$$(\epsilon_f)_{R_\beta} \cong \frac{\sigma_f^* - K^{max}_{\sigma(p)}\sigma_Y^*}{K^{max}_{\sigma(p)}\; d\sigma/d\epsilon} \tag{9}$$

Of course, both $K^{max}_{\sigma(p)}$ and σ_f^* will depend on strain somewhat in real materials, but no more exact analysis is possible at this time.

The plastic bend angle required to produce a strain ϵ_f at R_β below a notch of radius ρ is given by [34]

$$\theta_F = 800\,\rho R_\beta \epsilon_f \cong 800\,\rho R_\beta \left[\frac{\sigma_f^* - K^{max}_{\sigma(p)}\sigma_Y^*(T)}{K^{max}_{\sigma(p)}\; d\sigma/d\epsilon}\right] \tag{10}$$

θ_F increases slowly with temperature ($\sigma_Y^*\downarrow$) until the ductility transition T_N where it increases sharply. Unfortunately, almost all the previous studies of this transition have been performed on mild steel where the formation of stable cleavage microcracks modifies the notch geometry prior to final failure and complicates an analysis of the local fracture criteria. In addition, there is a concurrent initiation mode transition because the

notch strains at the ductility transition temperature are large enough (ϵ_f) to initiate fibrous tearing before unstable cleavage can occur. Consequently, the reason for this sharp increase in bend angle at T_N has not been completely understood [14]. Knott [5, 25] has proposed that it might be associated with plastic strain acting as a barrier to growth of microcrack nuclei [$\sigma_f^*\uparrow$, by crack blunting or increasing the steel's intrinsic toughness.] This, in turn, would increase the strain hardening required to reach σ_f^*, and the additional strain required would in turn raise σ_f^*, ϵ_f, and θ_F still more.

In the present work, Fe-Si was also studied because stable microcracks are not observed prior to unstable cleavage and fibrous tearing does not occur. In this case it is unlikely that the small plastic strains involved ($\epsilon_f < 10\%$) could increase σ_f^* sufficiently to produce the observed θ_F increase at the ductility transition. A more likely explanation is that the mechanics of deformation changes in one of two ways. First, a larger percentage of the bend angle can be accommodated by plastic zones which do not pass through the notch root or the region directly ahead of it. Consequently, a larger bend angle is required to produce a given notch strain, and the critical angle, θ_F equation (10), will be increased to

$$\theta_F = 800\,h\rho R_\beta \epsilon_f \tag{10a}$$

where h represents the fraction of the total bend angle which is accommodated without increasing the root strain. For example, the formation of 'plastic wings' in standard Charpy bars [35] allows continued bending without increased strain ahead of the notch. In general, h should increase with θ and be relatively independent of thickness. Secondly, extensive plastic deformation can occur through the thickness [$\chi(R,t)\downarrow$] thus increasing ϵ_F and θ_F.

The ductility transition is defined by the condition that

$$\theta_N = \theta_F\,(T)\;(T = T_N^t) \tag{11}$$

where θ_N is the angle at which either h, ϵ_f or σ_f^* increase markedly. The effect of thickness on the ductility transition temperature can be discussed in terms of its effect on θ_N and θ_F. Since θ_F increases from zero at the nil-ductility temperature (T_D) up to θ_N at the ductility transition (T_N), we may write

$$\theta_N = \frac{d\theta_F}{dT}\,(T_N - T_D) \tag{11a}$$

Because T_D varies with thickness, that same thickness dependence will appear in T_N even if θ_N and $d\theta_F/dT$ are thickness independent. Differentiating equation (10a)

$$\frac{d\theta_F}{dT} = 800\ h\rho R_\beta \frac{\Delta\epsilon_f}{\Delta T} = 800\ h\rho R_\beta \frac{d\sigma_Y^*/dT}{d\sigma/d\epsilon} \qquad (12)$$

Surprisingly, the increase of θ_F with temperature is independent of the maximum constraint and thus independent of thickness. On the other hand, extensive plane stress deformation occurs more easily in thinner bars so that θ_N decreases with decreasing thickness. When extensive plane stress deformation is responsible, the ductility transition should be even more thickness dependent than the nil-ductility temperature; this is experimentally observed in the Fe-Si bars. In mild steel, however, T_D and T_N show the same thickness dependence. Plane stress relaxation most certainly occurs, but it is masked by the formation of stable microcracks prior to failure. Equation (11a) is no longer applicable because of the effective change in geometry when microcracks form between T_D and T_N. The much sharper tip (ρ) accentuates stress intensification by strain hardening and increased strain rate, both of which are not reduced by plane stress deformation. Consequently, when stable microcracks are formed the ductility transition is less thickness dependent.

In drilled samples, two separate ductility transitions can be distinguished. Transition 1 results from relaxation of triaxiality by deformation through the thickness [$\chi(t,R)\downarrow$]; transition 2 results from the reduction of longitudinal stress and strain by in-plane deformation when tearing reaches both blunted holes, $K^{\infty}_{\alpha(\rho)}\downarrow$. In order to produce relaxation of plane strain conditions and allow transition 1, two criteria must be satisfied. The first requires that tearing reach one hole before cleavage occurs below the notch, i.e.

$$\theta_S^H < \theta_F^H \qquad \text{(criterion 1)} \qquad (13)$$

$$\frac{Const.}{\alpha}\ \epsilon_s < \alpha\ 800\ \rho R_\beta \epsilon_F^H \qquad (13a)$$

θ_S^H is the bend angle at which shear failure occurs between the notch side and one hole, and θ_F^H is the critical bend angle for cleavage fracture, analogous to equation (10) but with the maximum constraint for drilled bars. The strain redistribution parameter (α) represents the ratio of strain between the notch side and hole to that ahead of the notch. The second criterion necessary for transition 1 is that plane strain conditions be relaxed before cleavage occurs ahead of the one hole, i.e.

$$\theta_N(H) < \theta_F(H) \qquad \text{(criterion 2)} \qquad (14)$$

Equation (14) is analogous to equation (11) except that the 'H' denotes that the effective notch tip is a blunted hole. Due to the larger effective ρ and lower constraint, both criteria can be satisfied more easily (at a lower temperature) than equation (11) for the standard bars.

In Fe-Si, the shear failure strain ϵ_s is so high (no fibrous tearing) that criterion 1 is the more difficult to satisfy. However, because the hole is much blunter when shearing does occur, criterion 2 is easily satisfied. In mild steel, fibrous tearing occurs at a relatively small end angle θ_S^H, and criterion 2 is controlling. In both materials, holes reduce the ductility transition temperature in each thickness, but the reductions are smaller and thickness dependent in the Fe-Si where criterion 1 requires very large bend angles. In mild steel, where the second criteria controls behavior, the thickness dependence of T_N is quite small because most stress intensification is by strain hardening after tearing reaches one hole.

The second type of ductility transition 2 occurs when tearing reaches both holes. The effective notch then has two blunt tips from which fracture reinitiation requires extensive deformation [9]. Two criteria must also be satisfied for this transition to occur. First, tearing must reach one hole, and criterion 1 is again given by equation (13). Secondly, the critical bend angle for reinitiation of cleavage $\theta_F(H)$ at the hole must be sufficiently large to assure that tearing will reach the second hole. Tearing is experimentally observed to reach both holes at a temperature ($T_{N'H}$) which is independent of thickness. Because criterion 2 is controlling and the majority of stress intensification ahead of the blunted holes results from strain hardening, $T_{N'H}$ is thickness independent.

Conclusions

1. In Charpy V-notch bars of reduced thickness:
   a. Plastic constraint develops more slowly with applied load.
   b. The maximum constraint developed at general yield is considerably lower.
   c. Relaxation of constraint occurs at a smaller bend angle. These modifications have been shown to (a) increase the low temperature notch strength, (b) reduce the nil-ductility temperature, and (c) reduce the ductility transition temperature of thinner bars respectively.
2. Conditions of plane strain and high constraint are not necessary prerequisites for improvements from two drilled holes. In samples of reduced thickness, drilled holes produce similar changes in notch strength prior to general yielding, the nil-ductility temperature, and the behavior of fully ductile samples (P_{GY}, P_{ult}). Similar percentage reductions in the plastic constraint are produced in all thicknesses because holes redis-

tribute the in-plane, longitudinal strains away from the notch and do not depend on nor produce enhanced through-thickness strains.

3. In the ductility transition region, the improvements from two holes depend on both thickness and microstructure as described in the text.

References

1. IRWIN, G. R., KIES, J. A. and SMITH, H. L. *Proc. ASTM*, vol. 58, pp. 640-660, 1958.
2. DAVIS, S. O. 'Rev. of precracked Charpy fracture tough. testing tech.', AFML TR65-374, p. 11, Feb. 1968.
3. LEICHTER, H. L. *J. Spacecraft and Rockets*, vol. 3, no. 7, p. 1113, July 1966.
4. KAUFMAN, J. G. *Trans. ASME D*, vol. 89, no. 3, p. 503, Sept. 1967.
5. KNOTT, J. F. *Proc. Roy. Soc.*, vol. A 285, p. 150, April 1965.
6. SAKUI, S. *et al.*, *Iron Steel*, vol. 4, p. 672, 1963.
7. CASTRO, R. and GUEUSSIER, A. *Rev. Metal.*, vol. 46, p. 517, 1949.
8. ORNER, G. M., HARTBOWER, C. E. *Weld. J. Res. Suppl.*, p. 521S, Dec. 1957.
9. TETELMAN, A. S. and RAU, C. A. Jr. 'The effect of small drilled holes on the notch toughness of iron base alloys', *Proc. First Int. Conf. on Fract.*, vol. 2, p. 691, 1965.
10. RAU, C. A. Jr. 'The effect of drilled holes on notch toughness', Ph.D. Thesis, Stanford University, April 1967.
11. TANAKA, M. and UMEKAWA, S. *Proc. First Japan Cong. Test. Mat'ls.*, p. 95, 1958.
12. COTTERELL, B. *Brit. Welding J.*, vol. 9, p. 83.
13. AUGLAND, B. *Brit. Welding J.*, vol. 9, p. 434.
14. STONE, D. E. W. Ph.D. Thesis, London, 1963.
15. TARDIFF, H. P. and MARQUIS, H. *Canadian Met. Quart.*, vol. 2, p. 373.
16. FEARNEHOUGH, G. D. and HOY, C. J. *J. Iron and Steel Inst.*, vol. 202, p. 912, 1964.
17. RADON, J. C. and TURNER, C. E. 'Fracture toughness measurements by instrumented impact test', 2nd National Symposium on Fract. Mec., Lehigh Univ., June 1968.
18. RAU, C. A. Jr. and WILSHAW, T. R., to be published.
19. HILL, R. *Mathematical Theory of Plasticity*, Oxford, London, 1950.
20. WILSHAW, T. R. and PRATT, P. L. *J. Mech. Phys. Solids*, vol. 14, p. 7, 1966.
21. WILSHAW, T. R., RAU, C. A. Jr. and TETELMAN, A. S. *Engr. Fract. Mech.*, vol. 1, no. 1, p. 191, June 1968.
22. GREEN, A. P. and HUNDY, B. B. *J. Mech. Phys. Solids*, vol. 4, p. 128, 1956.
23. EWING, D. J. F. *J. Mech. Phys. Solids*, vol. 16, p. 205, 1968.
24. HENDRICKSON, J. A., WOOD, J. A. and CLARK, D. S. *Trans. ASM*, vol. 50, p. 656, 1958.
25. KNOTT, J. F. *J.I.S.I.*, vol. 204, p. 104, 1966.
26. WILSHAW, T. R. and PRATT, P. L. *Int. Conf. Fract., Sendai, Japan*, vol. B III, p. 3, 1965.
27. TETELMAN, A. S., WILSHAW, T. R., and RAU, C. A. Jr. 'Critical tensile stress criterion for cleavage', *Int. Symp. Fract. Mech.*, Kiruna, Sweden, Aug. 1967.
28. HAHN, G. T. and ROSENFIELD, A. R. *Trans. ASM*, vol. 59, p. 909, 1966.

29. KNOTT, J. F. *J. Mech. Phys. Sol.*, vol. 15, p. 97, 1967.
30. SMITH, E. *Acta Met.*, vol. 14, p. 985, Aug. 1966.
31. SMITH, E. *Ibid*, p. 991.
32. SMITH, E. and BARNBY, J. J. *Met. Sci. J.*, vol. 1, p. 56, 1967.
33. RAU, C. A. Jr. and TETELMAN, A. S. 'The effect of two drilled holes on the elastic and elastic-plastic strain distribution around a Charpy V-notch', (submitted to *Experimental Mechanics*).
34. TETELMAN, A. S. and WILSHAW, T. R., to be presented Second Int. Con. on Fracture, Brighton, 1969.
35. WILSHAW, T. R. *J.I.S.I.*, vol. 204, p. 936, 1966.

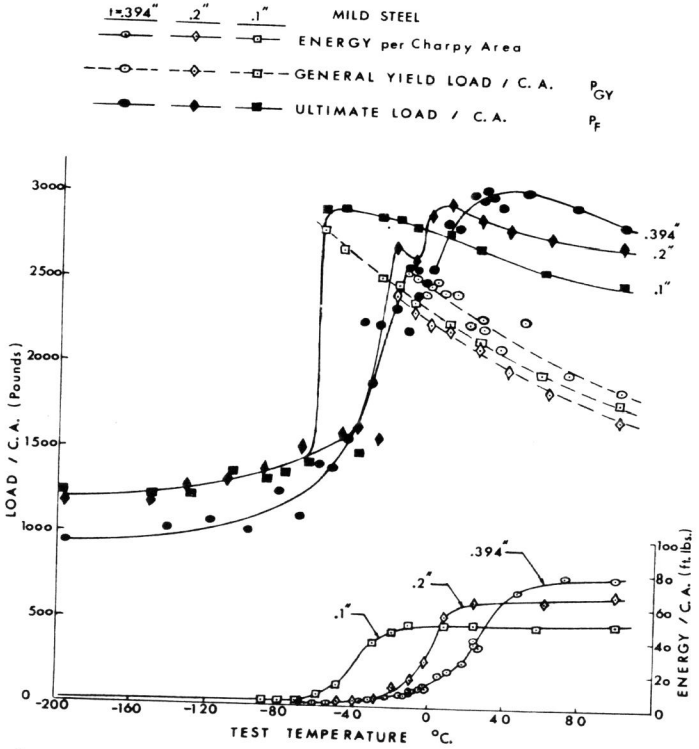

Fig. 1. Instrumented Charpy fracture results at various test temperatures for mild steel bars of various thickness (t = 0·1, 0·2, 0·394 in), all measured loads and energies have been normalized to the standard Charpy area.

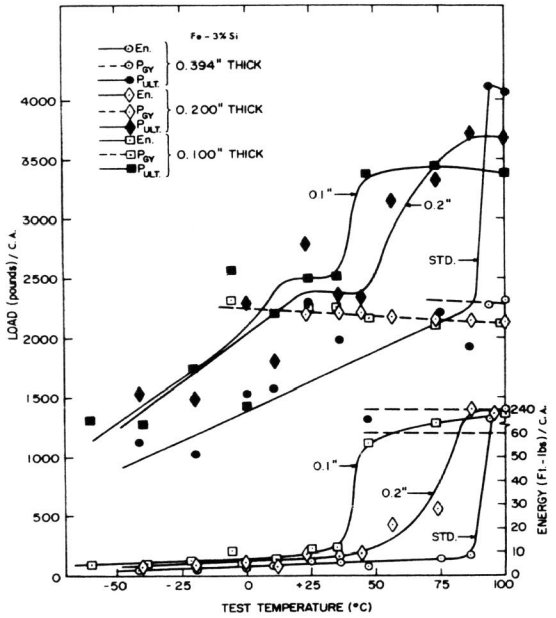

Fig. 2. Instrumented Charpy fracture results at various test temperatures for Fe-3% Si bars of three thicknesses (0·1, 0·2, and 0·394 in); all loads and energies are normalized to the standard Charpy area.

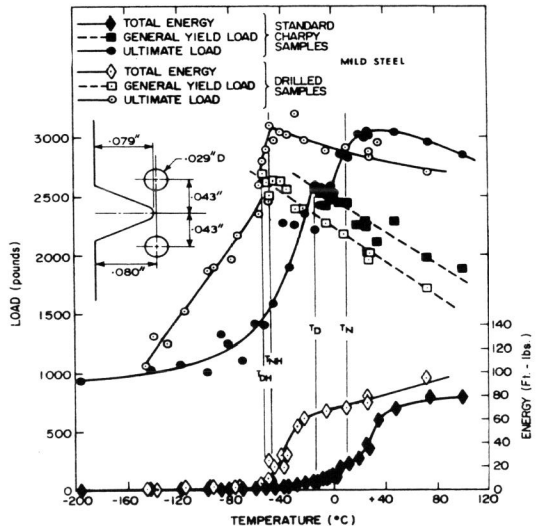

Fig. 3. The effect of two drilled holes on the instrumented Charpy fracture results for mild steel at various test temperatures.

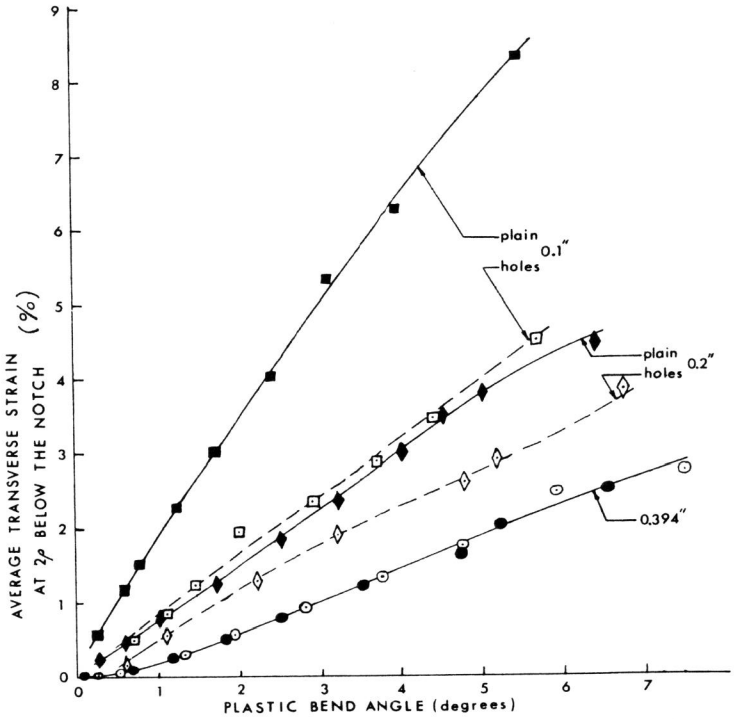

Fig. 4. The effect of specimen thickness and two holes on the average transverse strain present at two root radii (0·020 in) below the notch at various plastic bend angles.

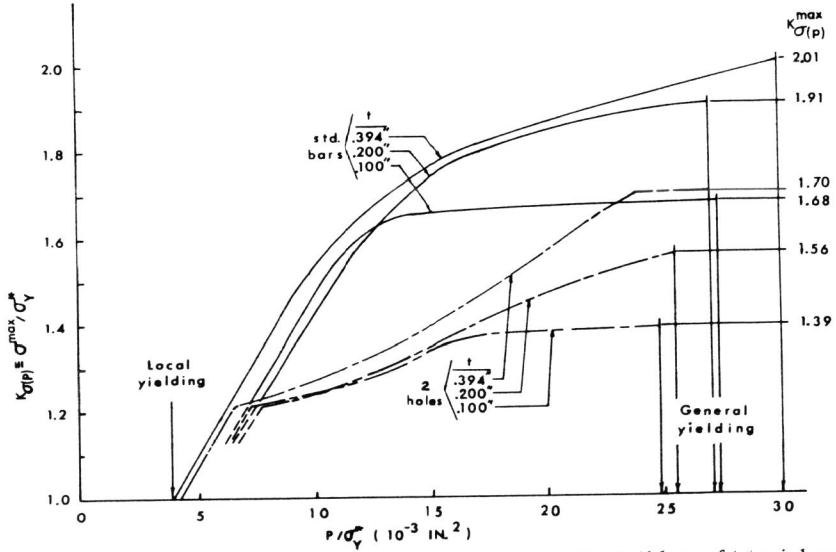

Fig. 5. The effect of specimen thickness and two holes on the build up of triaxial constraint with applied load and the maximum constraint produced in mild steel 'Charpy bars' the applied loads are normalized to the standard Charpy area.

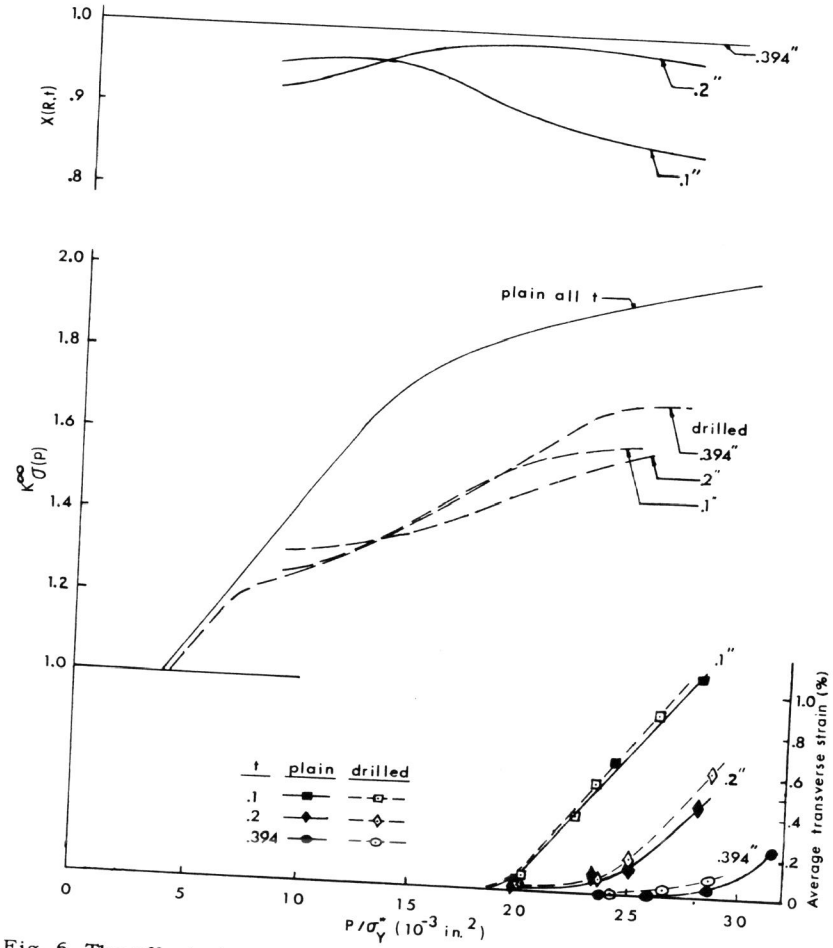

Fig. 6. The effect of specimen thickness and two holes on the average transverse strains and associated relaxation of plane strain conditions, $X(R, t)$, at various applied loads prior to general yielding all loads are normalized to the standard Charpy area.